

Coronary Artery Stenosis Quantification for Computed Tomography Angiography Based on Modified Student's t -Mixture Model

Qiaoyu Sun, Guanyu Yang, Huazhong Shu, and Daming Shi

Coronary artery disease (CAD) is a major cause of death in the world. As a non-invasive imaging modality, computed tomography angiography (CTA) is now usually used in clinical practice for CAD diagnosis. Precise quantification of coronary stenosis is of great interest for diagnosis and treatment planning. In this paper, a novel cluster method based on a Modified Student's t -Mixture Model is applied to separate the region of vessel lumen from other tissues. Then, the area of the vessel lumen in each slice is computed and the estimated value of it is fitted with a curve. Finally, the location and the level of the most stenoses are captured by comparing the calculated and fitted areas of the vessel. The proposed method has been applied to 17 clinical CTA datasets and the results have been compared with reference standard degrees of stenosis defined by an expert. The results of the experiment indicate that the proposed method can accurately quantify the stenosis of the coronary artery in CTA.

Keywords: Computed tomography angiography, Modified Student's t -Mixture Model, Soft plaque, Stenosis quantization, Vascular segmentation.

Manuscript received Dec. 12, 2016; revised May 26, 2017; accepted June 19, 2017.

Qiaoyu Sun (sunqy@hhit.edu.cn) are with the College of Electronic Engineering, Huaihai Institute of Technology, Lianyungang, Jiangsu, China.

Guanyu Yang (yang.list@seu.edu.cn) and Huazhong Shu (shu.list@seu.edu.cn) are with the LIST of the Department of Computer Science and Engineering of the Southeast University, Nanjing, Jiangsu, China.

Daming Shi (corresponding author, dshi@szu.edu.cn) is with the School of Computer Science and Software Engineering, Shenzhen University, China.

This is an Open Access article distributed under the term of Korea Open Government License (KOGIL) Type 4: Source Indication + Commercial Use Prohibition + Change Prohibition (<http://www.kogil.or.kr/news/dataView.do?dataIdx=97>).

I. Introduction

Coronary artery disease (CAD) is a major cause of death worldwide [1]. Computed Tomography Coronary Angiography (CTCA) is a frequently used modality for the detection of CAD as it visualizes the 3D course of the coronary arteries and shows a good correlation with the gold standard, conventional coronary angiography [2]. By observing the form of the lumen and wall of the coronary artery in coronary Computed Tomography (CT) images, cardiologists can determine the severity of stenosis and the type of the plaque (soft, calcium, and mixed plaque) [3]. However, quantitative measurement of the degree of stenosis largely depends on the manual delineation of the cardiologists, which may unavoidably lead to inter- and intra-observer variability. Therefore, a computer-aided diagnosis system should be developed to improve the efficiency of the cardiologists or radiologists and the accuracy of the diagnosis, while simultaneously reducing both inter- and intra-observer variability.

The number of publications presenting coronary artery stenosis detection and quantification methods have increased in recent years. Dey and others [4] proposed an automatic segmentation and quantification method named APQ. The calcified and non-calcified plaques are quantified and analyzed by some basic algorithms used in image processing. Dey and others [5] also used intravascular ultrasound (IVUS) to verify their method. Kelm and others [6] introduced a stenosis detecting system focusing on coronary CTA, which employed a nonlinear regression method to estimate the vessel diameter of a 2D vessel cross section to obtain the stenosis point of the vessel. Xu and others [7] presented a method for detecting and quantifying coronary arterial

stenosis in CTA using the Fuzzy Distance Transform (FDT) approach and developed a method to estimate the “expected diameter” along a given arterial branch using a coherence analysis. Rahil and others [8] presented a method to automatically detect and quantify coronary artery stenosis in CTCA. The expected diameter of the healthy lumen is estimated by applying robust kernel regression to the coronary artery lumen diameter profile. Stenosis is detected and quantified by computing the difference between estimated and expected diameter profiles. Medical Image Computing and Computer Assisted Intervention (MICCAI) 2012 sponsored the “3D Cardiovascular Imaging: a MICCAI segmentation challenge” workshop for coronary artery stenosis detection, stenosis quantification and lumen segmentation algorithms in CTA. Abouzar and others [9] proposed a coronary segmentation method by estimating the likelihood of transversal circles around the manually refined vessel LKEB centerline. Stenoses are detected and graded based on the observed and expected cross-sectional area of the vessel as well as the intensity profile of segmented lumen for quantification of stenosis with sub-pixel accuracy. A modified minimal path approach is used to extract a centerline between the artery endpoints in [10]. The stenoses are detected and quantified by comparing the reconstructed cylinder with an ‘idealized’ one based on a linear regression of the radii of the most reliable contours. Lor and others [11] developed a fully automated probabilistic approach in detecting and quantifying coronary artery plaque, which serves as evidence of luminal narrowing of the assessed degree. The quantitative evaluation of diameter stenosis is determined using the Kalman filtering formulation. The stenosis degree is given using the Bayes classifier based on the posterior probability of severity conditioned on the stenosis percentage and plaque type of the training data. Mohr and others [12] performed stenosis detection and quantification based on estimating the expected vessel profile at each point along the vessel. A line is fitted to the calculated vessel lumen diameters to provide an expectation of the lumen diameter at each position. The stenosis percentage is then calculated as the percentage deviation of the real lumen diameter from the expected one. Overall, most of the entries focused on stenosis detection. Kitamura and others [13] proposed a novel segmentation method based on multi-label graph cuts utilizing higher-order potentials to impose shape priors for coronary lumen and plaque segmentation in CT angiography. The Hessian analysis is used to detect the candidate shapes and introduce corresponding higher-order terms into the energy. Alizadehsani and others [14]

used analytical methods to investigate the importance of features on artery stenosis. Further, a classification model was built to predict each artery status in new visitors. To further enhance the models, a proposed feature selection method was employed to select more discriminative feature subsets for each artery. A number of rules with high confidence were introduced for deciding whether the arteries were stenotic.

As mentioned in [15], current stenosis quantification algorithms are not sufficiently reliable to be used by themselves in clinical practice, but could be used as a second-reader. The existing methods may have the following limits: 1) the quantification of the stenosis always depends on the result of the detection, and the detection is usually based on the result of vessel lumen segmentation, while the accuracy of the segmentation is not reliable because it is performed on all vessels. 2) The correct stenosis quantification requires suitable selection of the start and end points of the narrow. If the start and end points obtained from the detection stage are improper, the degree level may be too large or small even though some noise of regions close to a branch may be regarded as narrow and are quantified. Therefore, this work focuses on the accurate stenosis quantification of the interested coronary segment given by an expert in CTA data for clinical application. The vessel lumen of the interested segment is separated from the CTA data based on the Modified Student’s t-Mixture Model (MSMM) clustering method. Coronary stenosis quantification is performed according to the estimated value and the calculated vessel areas of each slice within the segment.

II. Materials/Patients

Seventeen CCTA images are acquired by a Siemens dual-source 64-slice CT scanner. The axial image size is 512×512 and the average axial resolution is ~ 0.33 mm. The distance between two axial slices is 0.5 mm. In these CCTA images, 30 stenoses were reported by radiologists. The grades of stenosis were measured by the radiologists with the Siemens syngo CT Coronary Analysis software. The grade of stenosis S_a is defined as

$$S_a = 100\% \times \left(1 - \frac{a_m}{a_r}\right), \quad (1)$$

where a_m is the minimal cross-sectional luminal area of a stenosis and a_r is the average cross-sectional luminal area at the begin and the end points of narrowing.

The grades of stenosis were measured by the radiologists with the Siemens syngo CT Coronary Analysis software. The ground truth of the stenosis quantification is given by

an expert. The stenosis ratios fall in the range of 0–100%. However, they have a relevant coarse step of 5%.

III. Methodology

This method focuses on coronary stenosis quantification based on the vessel lumen segmentation of an interested segment whose start point and end point are defined by an expert. The flowchart of our proposed method is shown in Fig. 1. Some preprocessing, that is cropping and thresholding, is employed to improve the efficiency of the method. The coronary lumen region is segmented by the MSMM method following a refinement. The quantification of stenosis is obtained by the calculated the vessel area of each cross sectional view, which can also indicate the most significant stenosis.

1. Preprocessing

The centerline of the coronary artery is extracted by the approach presented in [16].

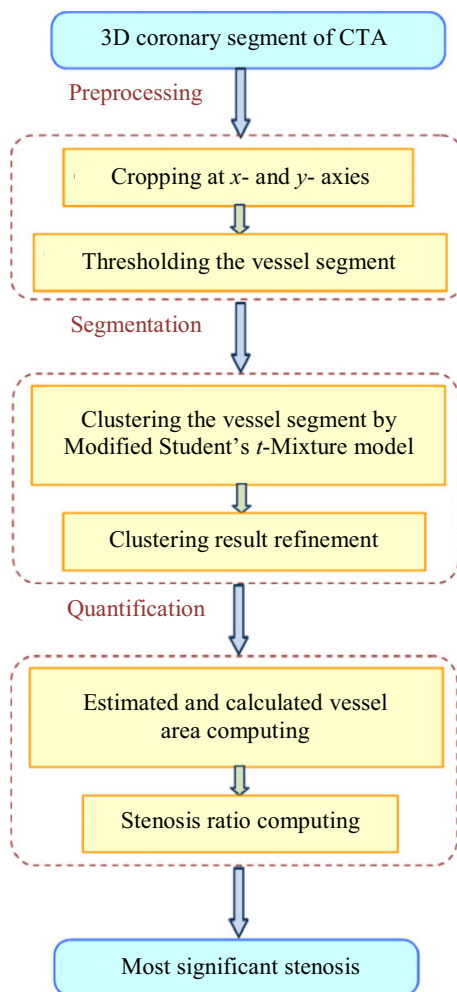


Fig. 1. Flowchart of the proposed method.

According to the points belonging to the centerline, a coronary artery can be straightened and reconstructed with 3D data and visualized in MeVisLab.¹⁾ A straight longitudinal image is a practical tool to display the morphology of a tortuous vessel extracted from a 3D image. In the straight longitudinal images, a change in the luminal diameter can be observed. The cross sectional view of the reconstructed coronary artery for our study has a resolution of $W \times H$. Figure 2 illustrates a longitudinal view of the front view and a cross sectional view of a reconstructed coronary artery starting from the aorta. The longitudinal view of the coronary with length L indicates that the vessel starts from aorta and its vessel diameter decreases from the proximal start to distal end. The cross sectional view corresponds to the location where the label *Coronary* points to.

A. Cropping

Consider that in a 2D cross-sectional view, the vessel is located at or very close to the center of the image and the biggest diameter of the coronary arteries is smaller than half of the width and half of the height of the cross sectional view, the vessel segment can be cropped in half on the x - and y - axis, as the yellow line indicates in Fig. 2.

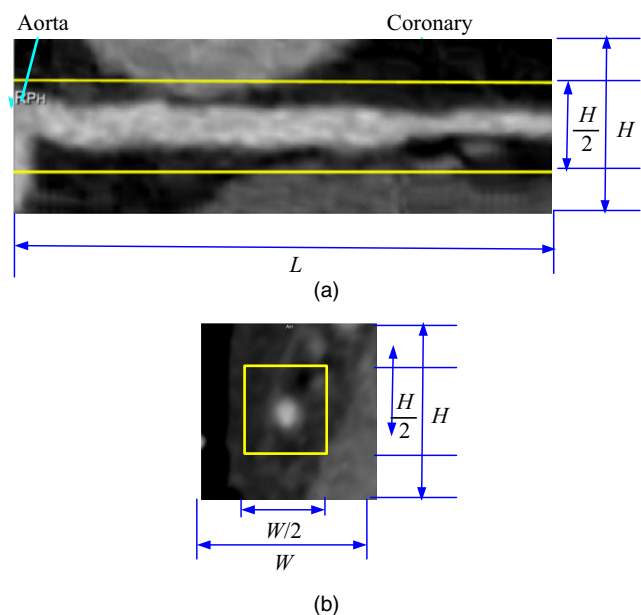


Fig. 2. Longitudinal and cross sectional view of a coronary artery: (a) longitudinal view of the coronary and (b) cross sectional view corresponds to the location where the label “Coronary” points to.

¹⁾ <http://www.mevislab.de/>

After the cropping, only quarter of the data needs to be processed, which may reduce the time consumption and remove some surrounding tissues.

B. Thresholding

As mentioned above, the cropped outside regions, which do not involve the vessels, may contain some surrounding tissues with similar intensities to the vessel region. However, this removal is not complete, because some vessels may be surrounded by myocardium or other tissues.

Then, a thresholding is applied on the cropped CTA data as follows:

$$g(w, h, l) = \begin{cases} f(w, h, l) & f(w, h, l) \geq T_1 \\ T_1 & \text{otherwise} \end{cases}, \quad (2)$$

where $f(w, h, l)$ and $g(w, h, l)$ denote the voxels of the origin data and the enhanced data, respectively. $w = 1, \dots, W; h = 1, \dots, H; l = 1, \dots, L$.

The thresholding can increase the value of the voxels corresponding to the dark region to further reduce the surrounding tissues. On the other hand, it decreases the values of the very bright voxels to remove the calcified plaque efficiently.

2. Lumen Segmentation based Modified Student's t-Mixture Model

The Student's t -Mixture Model (SMM), proposed by Peel and McLachlan as an alternative to the Gaussian Mixture Model (GMM), can provide high robustness against noise [17]. SMM is more robust than GMM for heavier tails, but neither GMM nor SMM take into account the spatial dependencies in the image. Moreover, they do not use the prior knowledge that adjacent pixels most likely have a high similarity. The Modified Student's t -Mixture Model based on the Finite Mixture Model (FMM) was presented for SAR image segmentation [18]. It incorporated the local spatial information and pixel intensity value by considering the conditional probability of an image pixel influenced by the probabilities of pixels in its immediate neighborhood.

A. Modified Student's t-Mixture Model

The Student's t -distribution provides a heavy-tailed alternative to the Gaussian distribution for potential outliers. The Probability Density Function (PDF) of a multivariate Student's t -distribution, with mean μ , covariance matrix Σ , and degrees of freedom ν , is [19]

$$t(y|\mu, \Sigma, \nu) = \frac{\Gamma(\nu/2 + p/2) |\Sigma|^{-1/2}}{\Gamma(\nu/2) (\pi\nu)^{p/2}} \left[1 + \frac{(y-\mu)^T \Sigma^{-1} (y-\mu)}{\nu} \right]^{-(\nu+p)/2}, \quad (3)$$

where p is the dimensionality of the variable y and $\Gamma(s)$ is the Gamma function $\Gamma(s) = \int_0^\infty t^{s-1} e^{-t} dt$.

For image segmentation, N pixels of an image will be segmented into K classes. y_i ($i = (1, 2, \dots, N)$) denotes the intensity value at the i -th pixel of an image $Q = \{1, 2, \dots, K\}$ and x_i denotes the corresponding class label ($I = \{1, 2, \dots, D\}$) of the i -th pixel.

When $x_i = j$ ($j = 1, 2, \dots, K$), y_i follows the conditional probability distribution selected as a Student's t -distribution. FMM can be expressed as [17]:

$$p(y_i|\pi, \theta) = \sum_{j=1}^K \pi_j p(y_i|\theta_{x_i}). \quad (4)$$

The Modified Student's t -Mixture Model modifies FMM with a mean filter to improve its robustness to noise. The spatial information for pixel i is incorporated to prior probability π_j , and the conditional probability of the i -th pixel $p(y_i|\theta_j)$ is influenced by the probability in its immediate neighborhood. Therefore, the modified SMM will be:

$$p(y_i|\pi, \theta) = \sum_{j=1}^K \pi_{ij} \left[t(y_i|\theta_j) \prod_{m \in \partial_i} t(y_m|\theta_j)^{\frac{\alpha}{N_i-1}} \right]^{\frac{1}{1+\alpha}}. \quad (5)$$

The Student's distribution $t(y_i|\theta_j)$ defined in (3) with parameters $\theta_j = \{\mu_j, \Sigma_j, \nu_j\}$ is as follows:

$$t(y_i|\theta_j) = t(y_i|\mu_j, \Sigma_j, \nu_j) = \frac{\Gamma(\frac{\nu_j}{2} + \frac{p}{2}) |\Sigma_j|^{-1/2}}{\Gamma(\frac{\nu_j}{2}) (\pi\nu_j)^{p/2}} \left[1 + \frac{(y_i - \mu_j)^T \Sigma_j^{-1} (y_i - \mu_j)}{\nu_j} \right]^{-\frac{(\nu_j+p)}{2}}. \quad (6)$$

B. Vessel Segmentation with MSMM

Vessel segmentation is an essential step of this work as the accuracy of quantification directly depends on the segmentation result. The Modified Student's t -Mixture Model is adopted to separate the vessel lumen from the interested segment.

In our work, the neighborhood window size of mean filter is selected as 3×3 and the number of iterations is 10. The number of the cluster is 2 which means that the voxel data of the coronary segment defined by the

proximal start and the distal end points will be clustered into two types: “vessel lumen” and “background.”

Figure 3 depicts the longitudinal view of a coronary vessel that has a significant stenosis. The start and end positions, L_S and L_E , indicate the region of the interesting segment which is labeled with two yellow lines. The cross sectional view of clustering results at three special locations which correspond to L_S , L_M and L_E , respectively. L_M is the most significant stenosis. The boundary of the vessel region obtained from the clustering method is depicted by a white curve.

C. Segmentation Refinement

In case the stenosis is located at the segment with a sub-branch as shown in Fig. 4, the branch vessel is usually assigned as an object according to the classification, which may lead to inaccurate stenosis quantification. Figures 4(a) and (b) show the longitudinal view of the interested segment and its 3D plots reconstructed according to the clustering result.

In general, the diameter of the lumen in adjacent cross sectional images will change gradually. Therefore, the clustering results influenced by the sub-branch can be refined using the estimated diameter of the vessel according to the clustering results obtained in the neighbored slices. A circle with diameter D_{eval} will be defined to remove the lumen belonging to the sub-branch. The predicted diameter $D_{eval}(l)$ in the l -th slice is defined as follows:

$$D_{eval}(l) = \begin{cases} \lambda * RL_l(\varphi_{min}) & RL_l(\varphi_{min}) \in [\beta_1 \sim \beta_2] * D_{eval}(l-1) \\ D_{eval}(l-1) & \text{otherwise} \end{cases} \quad (7)$$

Where λ is a coefficient decided empirically to ensure the circle can covers the entire lumen region, because the center of the vessel sometimes may vary a little from that of the image in the cross-sectional image. $RL_l(\varphi_i)$ is the run length from the center of the slice to the boundary of the lumen at four different orientations, That is $\varphi_i = i * 90^\circ, i = 0-3$. $RL_l(\varphi_{min}) = \min_i(RL_l(\varphi_i))$ denotes the smallest of the four run-lengths. Two parameters β_1 and β_2 determine a range that restricts $RL_l(\varphi_{min})$ to avoid yielding a predicated diameter that is too large or too small due to noise or stenosis.

The refinement can efficiently remove the branch and reduce the interference caused by the branch, as illustrated in Fig. 4(c).

Figure 5 illustrates the refinement procedure in cross-sectional image. Figure 5(a) illustrates the original

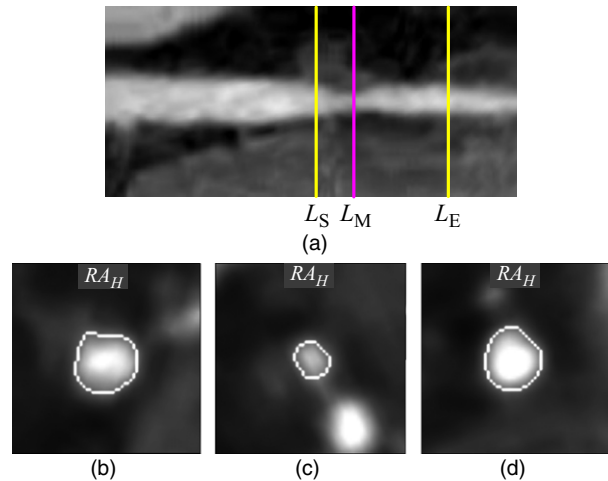


Fig. 3. Segmentation result by MSMM of a typical coronary artery segment. (a) Longitudinal view of the coronary artery, (b-d) Segmentation results at the start (L_S), end (L_E) and the most stenosis (L_M) positions labeled in cross sectional view.

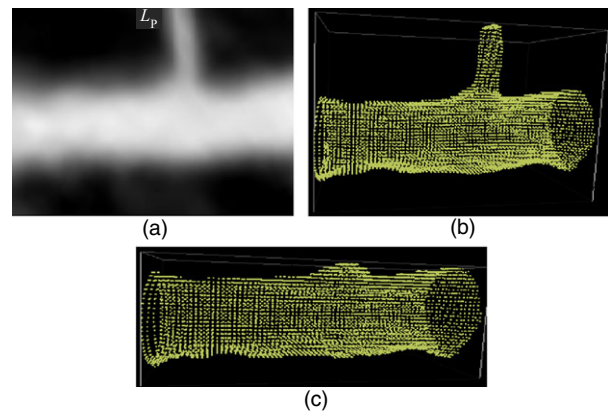


Fig. 4. Comparison of the original and refined clustering results: (a) vessel segment, (b) 3D plot of the original clustering result, and (c) 3D plot of the refined clustering result.

classified result in a cross-sectional image at a vessel branch whose boundary is enclosed by a red curve. Figure 5(b) shows the run lengths of the center point indicated by yellow arrows and their minimal length is labeled by a pink colored bidirectional arrow. The predicted diameter D_{eval} of the slice is determined by (7) and is depicted by a green circle covering Fig. 5(a), as shown in Fig. 5(c). After refinement, the region of sub-branch is removed and the detected lumen is more close to the real vessel region, as shown in Fig. 5(d). The lumen area of each slice will be calculated according to the clustering result and the predicted diameter, which can remarkably reduce the error of the calculated lumen area.

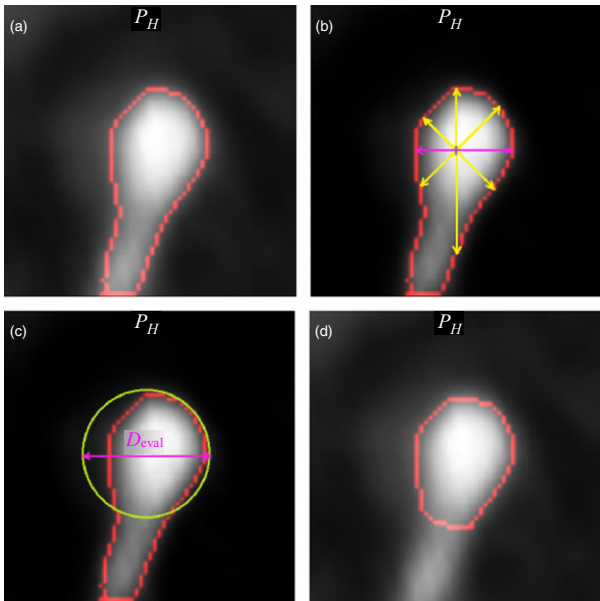


Fig. 5. Clustering result refinement: (a) clustering result, (b) run lengths at four orientations of the center point, (c) clustering result covered with the refined region determined by the predicted diameter, and (d) refined result.

3. Stenosis Quantification

The refined clustering result is employed to calculate the vessel area of each slice which is shown by a plot composed of blue crosses in Fig. 6. In order to be more intuitive, the longitudinal view of the interesting segments with the specific positions (L_S

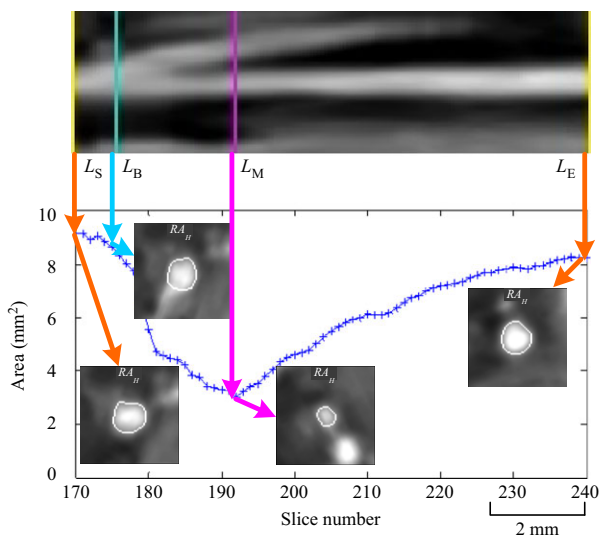


Fig. 6. Calculated vessel lumen area curve and the segmentation results in cross sectional view corresponding to the positions of the segment of interest.

L_M , L_B and L_E) are indicated using arrows with the corresponding cross sectional view segmentation results.

Consecutively, the minimal lumen area (MLA) of the stenosis is assessed using the difference between the calculated and the estimated lumen areas of the interested segment of the coronary artery [20]. The calculated lumen areas of each slice are denoted with green crosses in Fig. 7. L_M is the location of the most significant stenosis. $A_{est}(L_M)$ and $A_{cal}(L_M)$ are the estimated and calculated lumen areas of L_M .

The stenosis ratio $ST_{Area}(l)$ at slice l of a segment is calculated as follows:

$$ST_{Area}(l) = \frac{A_{est}(l) - A_{cal}(l)}{A_{est}(l)} = 1 - \frac{A_{cal}(l)}{A_{est}(l)}, \quad (8)$$

where $A_{est}(l)$ and $A_{cal}(l)$ are the estimated and calculated lumen cross-sectional areas of the interested segment at the i th slice.

The most significant stenosis of the segment is

$$ST_M = \max(ST_{Area}(l)), \quad for \quad l = 1, \dots, L_E - L_S + 1. \quad (9)$$

The stenosis quantification and the most significant stenosis detection of the interested segment in Fig. 6 are illustrated in Fig. 7. A slope is defined between the real areas relating to the endpoints of the interested segment that represents estimated the vessel areas of the normal proximal-to-distal tapering of the segment of interest, which is discretized and depicted by red star, while the calculated lumen area of each cross sectional image is denoted by green crosses. The location of the most significant stenosis L_M is labeled on the plot of the vessel areas. $A_{est}(L_M)$ and $A_{cal}(L_M)$ are the estimated and the calculated vessel areas of L_M , respectively.

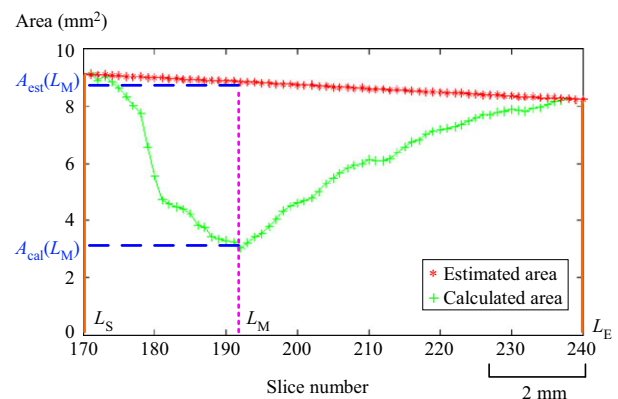


Fig. 7. Estimated (red ‘*’) and calculated (green ‘+’) vessel area curves of the segment in Fig. 4.

The proposed method also can handle the most significant stenosis of the mixed plaque. Figure 8 shows the longitudinal view of a coronary segment that contains a long mixed stenosis, two calcified plaques and some soft plaques. After the thresholding, the calcified plaque will be excluded from the lumen region, which results in lumen area reduction, as shown in the cross sectional lumen area curve of Fig. 8. The narrowest calcified plaque point, which is also the most significant position (L_M), and the local narrowest stenosis caused by one calcified and one noncalcified plaque of the segment of interest are mapped to the area curve accompanying the corresponding cross sectional view of the clustering result indicated by brown arrows. Figure 8 illustrates the longitudinal view of the interested segment and its lumen area curve of each slice (green crosses).

From the examples of the two typical coronary segments, we can find the efficiency of the proposed method for all kinds of plaques.

IV. Results

In order to demonstrate the validity of the proposed method, it is tested on seventeen patients whose CTA images were acquired by a Siemens dual-source 64-slice CT scanner. In these CTA images, 30 stenoses were reported by radiologists. The start and end points of the stenosis are labeled by the expert. According to these positions, the coronary artery is cut to a segment that mostly contains the stenosis. Our method used these segments for accurate quantification of the stenosis. Some

parameters in the experiments are chosen empirically; for example, T_1 in (2) is 1150. λ , and β_1 and β_2 in (7) are set to 1.2, 0.8 and 1.2, respectively.

Table 1 shows the most significant stenosis ratio results of all the 30 coronary segments compared with their ground truth decided by an expert.

The error of the proposed method for calculating the stenosis ratios of segment n is defined as the difference between the most significant stenosis $ST_M(n)$ quantified by the proposed method and the ground truth $ST_{MGT}(n)$ given by the expert:

Table 1. Respective results of the most significant stenosis level for all coronary segments compared with their ground truth.

No.	Data	ST_{MGT} (%)	ST_M (%)	Error (%)
1	P1-LAD	40	43.04	3.04
2	P2-LAD	50	47.92	2.08
3	P3-LAD	60	57.74	2.26
4	P3-RCA	45	42.42	2.58
5	P4-LAD	55	54.36	0.64
6	P5-LAD	15	16.58	1.58
7	P5-RCA	35	35.63	0.63
8	P6-LCX	35	35.06	0.06
9	P6-LAD	20	21.72	1.72
10	P6-RCA	35	34.74	0.26
11	P7-LAD	40	39.2	0.8
12	P7-RCA	25	36.68	11.68
13	P7-LCX	45	42.21	2.79
14	P8-LAD	55	48.44	6.56
15	P9-LAD	60	65	5
16	P10-LAD	40	39.07	0.93
17	P11-LCX	90	100	10
18	P11-LAD	60	60.88	0.88
19	P11-LAD	55	51.63	3.37
20	P12-LAD	25	30.8	5.8
21	P12-LAD	65	65.78	0.78
22	P13-LAD	50	50.64	0.64
23	P14-RCA	40	40.98	0.98
24	P14-DA	30	33.25	3.25
25	P15-LAD	40	40.15	0.15
26	P15-RCA	40	41.29	1.29
27	P16-RCA	90	100	10
28	P17-LM	35	35.41	0.41
29	P17-RCA	70	73.47	3.47
30	P17-RCA	70	65.32	4.68

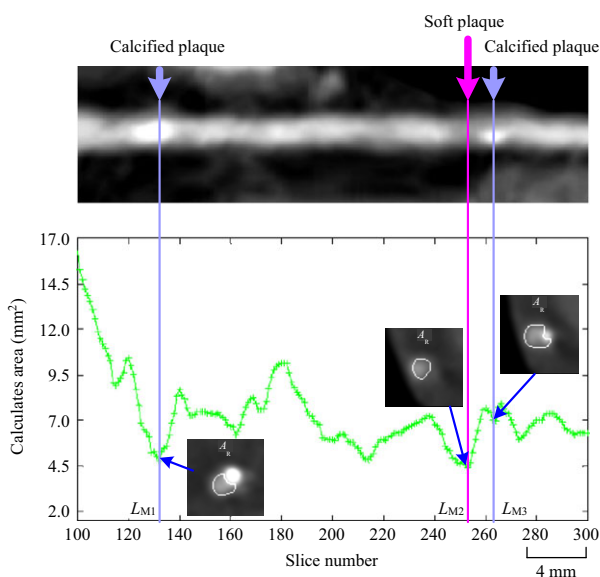


Fig. 8. Result of a coronary segment containing mixed plaque.

$$Error(n) = |ST_M(n) - ST_{MGT}(n)|. \quad (10)$$

In Table 1, the largest error (11.68%), existing on P7-RCA, is a calcified plaque (as Figure 8 shows).

Therefore, the absolute average difference (*AAD*) and the root mean squared difference (*RMSD*) of the proposed method for the dataset will be:

$$ADD = \frac{\sum_{n=1}^N Error(n)}{N}, \text{ for } n = 1, \dots, N, \quad (11)$$

$$RMSD = \sqrt{\frac{\sum_{n=1}^N Error(n)^2}{N}}, \text{ for } n = 1, \dots, N, \quad (12)$$

where *N* is the number of the stenosis in the test dataset. The *AAD* and *RMSD* of the stenosis ratio are about 2.94% and 4.24%, respectively.

Each stenosis can be assigned to the corresponding stenosis degree (mild, moderate, severe, and occluded) by applying QCA stenosis thresholds of less than 20% (< 20%), greater than 20% (≥ 20% and < 50%), greater than 50% (≥ 50% and < 70%), and greater than 70% (≥ 70%), respectively [15]. Table 2 gives the confusion matrix comparing agreements of stenosis quantification by the proposed method and an expert. Compared to the stenosis level results estimated by the experts, the proposed method missed two severe stenoses to a moderate degree and one occluded stenosis to a severe degree. For the formal two stenosis ratios quantified by the proposed method, the errors are 2.08% and 6.56%, respectively (see P2-LAD and P8-LAD in Table 1). For the latter one, the error is 4.68% (see P17-RCA in Table 1).

Table 2. Confusion matrix of stenosis quantification by the proposed method and an expert.

		Grade of stenosis by expert			
		Mild	Moderate	Severe	Occluded
Grade stenosis by our method	Mild	1			
	Moderate		16		
	Severe		2	7	
	Occluded			1	3

Table 3. Performance comparison between the proposed method and the method in [21].

Method	<i>AAD</i> (%)	<i>RMSD</i> (%)
Proposed method	2.94	4.24
Method in [21]	12.22	14.64

The performance of the proposed method is compared with the method of [21] in Table 3. The compared method applied Fuzzy C Means to segment the coronary artery from the CT images. From Table 3, we can find that the performance of the proposed method based on MSMM is better. Most stenosis ratio results of the method in [21] are higher than their ground truth more or less, which may result in a lower performance.

V. Discussion

Our method is an accurate quantification method for coronary artery stenosis with CTA data. Different from other existing quantification methods, the proposed method quantifies the stenosis according to the interested segment defined by an expert but not the detected segment, which may or may not contain the stenosis. The preliminary experimental results are well consistent with the reference standards. These can be provided to the radiologist or cardiologist for accurately evaluating the degree of the stenosis.

The proposed method is evaluated by the interested segments mainly located in the proximal and middle part of the coronary arteries. Owing to the partial volume effect, the feasibility of our method for the segments on the distal parts needs to be verified in future. Moreover, the number of datasets for evaluation is relatively small, and is composed of 30 segments of interest for 17 patients. A further validation with a large number of clinical datasets will be performed in future. Considering the X-ray angiography and IVUS are always used as accurate references for clinical stenosis quantification, the proposed method will be verified using X-ray angiography or IVUS for further more accurate evaluation.

VI. Conclusion

Lumen segmentation of coronaries is one of the key techniques of the CAD computer-aided diagnosis that is based on the coronary CTA. With the popularization of the 64-slice CT, segmented approaches involving the lumen and plaques of coronary in CTA have been the focus of research. The area of the plaque region or the volume of the lumen can be obtained by segmentation, and then, the vascular remodeling index and stenosis index can be calculated. Both of them have important significance for clinical treatment. A simple stenosis quantification method for coronary in CTA image is proposed in this paper. After some needful preprocessing, a commonly cluster approach FCM was employed to distinguish the “vessel” from the background of an interested segment with given endpoints.

A refining process was applied for more accurate segmentation. The stenosis quantification of the vessel segment was completed by computing the vessel area of each slice according to the clustering result. The most significant stenosis was detected by comparing the estimated and calculated vessel area of each slice. The method was tested on a special dataset and the efficiency for the coronary artery stenosis quantification was verified by both calcified and noncalcified plaques.

Acknowledgements

This research was supported by the National Basic Research Program of China under grant (2011CB707904), National Natural Science Foundation under grants (81101104, 61271312), Natural Science Foundations of Jiangsu Province (BK2012743), Six talent peaks project of Jiangsu Province (2012 DZXX-031), and Postdoctoral scientific research funding scheme of Jiangsu Province (1302018C).

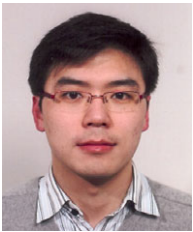
References

- [1] V.L. Roger et al., "Heart Disease and Stroke Statistics—2012 Update: A Report From the American Heart Association," *Circulation*, vol. 125, no. 1, 2012, pp. 2–220.
- [2] S. Leschka et al., "Accuracy of MSCT Coronary Angiography With 64-Slice Technology: First Experience," *Eur. Heart J.*, vol. 26, no. 15, 2005, pp. 482–487.
- [3] M. Naghavi et al., "From Vulnerable Plaque to Vulnerable Patient: A Call for New Definitions and Risk Assessment Strategies: Part I," *Circulation*, vol. 108, no. 14, 1980, pp. 1664–1672.
- [4] D. Dey et al., "Automated 3-Dimensional Quantification of Noncalcified and Calcified Coronary Plaque from Coronary CT Angiography," *J. Cardiovasc. Comput. Tomogr.*, vol. 3, no. 6, 2009, pp. 372–382.
- [5] D. Dey et al., "Automated Three-Dimensional Quantification of Noncalcified Coronary Plaque From Coronary CT Angiography: Comparison With Intravascular US," *Radiology*, vol. 257, no. 2, 2010, pp. 516–522.
- [6] B.M. Kelm et al., "Detection, Grading and Classification of Coronary Stenoses in Computed Tomography Angiography," *Med. Image Comput. Comput. Assist. Interv. (III)*, Toronto, Canada, Sept. 2011, pp. 25–32.
- [7] Y. Xu et al., "Quantification of Coronary Arterial Stenoses in CTA Using Fuzzy Distance Transform," *Comput. Med. Imaging Graph.*, vol. 36, no. 1, Jan. 2012, pp. 11–24.
- [8] R. Shahzad et al., "Automatic Segmentation, Detection and Quantification of Coronary Artery Stenoses on CTA," *Int. J. Cardiovasc. Imaging*, vol. 29, no. 8, Dec. 2013, pp. 1–13.
- [9] A. Abouzar et al., "Quantification of Coronary Arterial Stenosis by Inflating Tubes in CT Angiographic Images," *MICCAI Workshop 3D Cardiovascular Imaging: ICCAI Segmentation Challenge*, Nice, France, Oct. 2012.
- [10] L. Florez-Valencia et al., "Coronary Artery Segmentation and Stenosis Quantification in CT Images With Use of a Right Generalized Cylinder Model," *MICCAI Workshop 3D Cardiovascular Imaging: MICCAI Segmentation Challenge*, Nice, France, Oct. 2012.
- [11] K.L. Lor et al., "Probabilistic Model Based Evaluation of Coronary Artery Stenosis on CTA," *MICCAI Workshop 3D Cardiovascular Imaging: MICCAI Segmentation Challenge*. Nice, France, October, 2012.
- [12] B. Mohr, S. masood, and C. Plakas, "Accurate Stenosis Detection and Quantification in Coronary CTA," *MICCAI Workshop 3D Cardiovascular Imaging: MICCAI Segmentation Challenge*, Nice, France, October, 2012.
- [13] Y. Kitamura et al., "Coronary Lumen and Plaque Segmentation from CTA Using Higher-Order Shape Prior," *Med. Image Comput. Comput. Assist. Interv. (XVII)*, Cambridge, USA, October, 2014, pp. 339–347.
- [14] R. Alizadehsani et al., "Coronary Artery Disease Detection Using Computational Intelligence Methods," *Knowl.-Based Syst.*, vol. 109, no. C, Oct. 2016, pp. 187–197.
- [15] H.A. Kirisli et al., "Standardized Evaluation Framework for Evaluating Coronary Artery Stenosis Detection, Stenosis Quantification and Lumen Segmentation Algorithms in Computed Tomography Angiography," *Med. Image Anal.*, vol. 17, no. 8, 2013, pp. 859–876.
- [16] G. Yang et al., "Automatic Centerline Extraction of Coronary Arteries in Coronary Computed Tomographic Angiography," *Int. J. Cardiovasc. Imaging*, vol. 28, no. 4, Apr. 2012, pp. 921–933.
- [17] D. Peel, and G.J. McLachlan, "Robust Mixture Modeling Using the t-Distribution," *Stat. Comput.*, vol. 10, no. 4, Oct. 2000, pp. 335–344.
- [18] H. Zhang et al., "Synthetic Aperture Radar Image Segmentation by Modified Student's t-Mixture Model," *IEEE Trans. Geosci. Remote*, vol. 52, no. 7, July 2013, pp. 4391–4403.
- [19] G. McLachlan, and D. Peel, *Finite Mixture Models*, New York, USA: John Wiley and Sons, 2000.
- [20] A. Broersen et al., "FrenchCoast: Fast, Robust Extraction for the Nice Challenge on Coronary Artery Segmentation of the Tree," *MICCAI Workshop 3D Cardiovascular Imaging: MICCAI Segmentation Challenge*, Nice, France, Oct. 2012.
- [21] Q. Sun, G. Yang, and H. Shu, "Stenosis Quantification of Coronary Artery CTA Images Based on Fuzzy C-Means Algorithm," *J. Southeast Univ.*, vol. 46, no. 1, Jan. 2016, pp. 30–34.



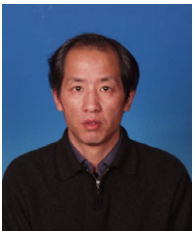
Qiaoyu Sun received the BS degree in electrical automation from Tianjin University, China, and the MS and Ph.D. degrees in computer application technology from East China Normal University, Shanghai, China, in 2003 and 2012, respectively. She is now with the

College of Electronic Engineering, Huaihai Institute of Technology, Lianyungang, China. Her research interests include document image recognition and retrieval, natural language processing, biometrics, and intelligent system development.



Guanyu Yang received the BS and MS degrees in biomedical engineering from Southeast University, Nanjing, China, in 2002 and 2004 respectively, and a PhD degree in signal processing and telecommunications from the University of Rennes 1, France, in 2008. He was a

postdoctoral fellow with the division of image processing, Leiden University Medical Center, Leiden, the Netherlands, from 2009 to 2011. He is now with the LIST of the Department of Computer Science and Engineering of the Southeast University. His research interest mainly focuses on medical image analysis and pattern recognition.



Huazhong Shu (M'00–SM'06) received the BS degree in Applied Mathematics from Wuhan University, China, in 1987, and a Ph.D degree in Numerical Analysis from the University of Rennes 1, France, in 1992. He is a professor at the LIST

Laboratory and the co-director of the CRIBs. His recent work concentrates on image analysis, pattern recognition, and fast algorithms in digital signal processing. Prof. Shu is a senior member of the IEEE Society.



Daming Shi received the PhD degree in mechanical engineering from Harbin Institute of Technology, China, in 1997, and the PhD degree in computer science from University of Southampton, United Kingdom, in 2002. Before he joined Shenzhen University as a Distinguished

Professor in 2016, he had been serving as a Reader / Professor at Middlesex University, UK, since 2010, and Assistant Professor at Nanyang Technological University, Singapore, during 2002–2009. His current research interests include machine learning, image processing and computer vision.